Computations. Least-squares curve fitting was accomplished on a Control Data Corp. Cyber 170 Model 750 computer using the KINFIT program developed by Dye and Nicely.[45] The procedures and subroutines used to fit the ethidium binding results were analogous to those developed by Mei et al.[46] for fitting multiple metal ion complexation equilibria to NMR chemical shift data.

Acknowledgment. The partial support of this research by NIH Grant GM-23516 is gratefully acknowledged.

Registry No. II, 3546-21-2; 5′-GMP, 85-32-5; Na, 7440-23-5; K, 7440-09-7.

---

(45) Dye, J. L.; Nicely, V. A. *J. Chem. Educ.* **1971**, *48*, 443.

(46) Mei, E.; Dye, J. L.; Popov, A. I. *J. Am. Chem. Soc.* **1977**, *99*, 5308.

(47) **Note Added in Proof:** Recently Petersen et al.[48] have interpreted the ^{1}H, ^{13}C, and ^{31}P NMR spectral properties of ordered Na$_2$(5′-GMP) in terms of stacked H-bonded dimers. Their dimer model may be ruled out on the basis of the stoichiometric results of the present paper and the previously reported ^{13}C NMR results[15] which provide an estimate of the size of an ordered aggregate.

(48) Petersen, S. B.; Led, J. J.; Johnston, E. R.; Grant, D. M. *J. Am. Chem. Soc.* **1982**, *104*, 5007.

Structure and Stereochemical Nonrigidity in Pd(F$_6$acac)$_2$P(aryl)$_3$, a New Isomeric Class of Palladium Bis(hexafluoroacetylacetonate) Complexes

A. R. Siedle,* R. A. Newmark, and L. H. Pignolet

Contribution from the 3M Central Research Laboratory, St. Paul, Minnesota 55101, and the Department of Chemistry, University of Minnesota, Minneapolis, Minnesota 55455.

Received November 30, 1981

Abstract: The reaction of palladium bis(hexafluoroacetylacetonate), Pd(F$_6$acac)$_2$, and (aryl)$_3$P produces Pd(F$_6$acac)$_2$P(aryl)$_3$, a new class of 1:1 adducts isomeric with carbon-bonded Pd(F$_6$acac-*C*)(F$_6$acac-*O,O*)(ligand). Pd(F$_6$acac)$_2$PPh$_3$ crystallizes in the monoclinic space group $P2_1/n$ with $a = 20.106$ (3) Å, $b = 13.160$ (7) Å, $c = 23.185$ (3) Å, $\beta = 93.52$ (3)°, and $V = 6123$ (5) Å^3. The structure solution, which converged at $R = 0.071$ and $R_w = 0.086$ with 6536 reflections for which $F_o^2 \geq 2.0\sigma(F_o^2)$, showed that the palladium has a distorted, square-pyramidal coordination geometry. The base of the pyramid comprises a phosphorus atom, two oxygen atoms from a bidentate F$_6$acac, and one oxygen atom from a semichelating F$_6$acac. The Pd–O contact involving the apical oxygen, provided by the other terminus of the semichelating F$_6$acac, is long, 2.699 (6) Å. The Pd(F$_6$acac)$_2$P(aryl)$_3$ compounds are stereochemically nonrigid, and the barrier to rearrangement increases as the steric bulk of the (aryl)$_3$P group increases. At low temperatures, the ^{19}F NMR spectrum of Pd(F$_6$acac)$_2$P(*o*-tolyl)$_3$ displays four singlets of equal area. These simultaneously coalesce at ca. −40 °C, indicative of a single dynamic process involving a C_{2v} square-pyramidal transition state in which all four CF$_3$ groups are equivalent. Analysis of the DNMR spectra gave $\Delta H^\ddagger = 7.7 \pm 1$ kcal/mol and $\Delta S^\ddagger = -20 \pm 5$ eu. Comparison of the molecular structures of the Ph$_3$P and (*o*-tolyl)$_3$P adducts of Pd(F$_6$acac)$_2$ suggests that the less bulky triphenylphosphine ligand is associated with geometrical changes that may parallel those associated with formation of the transition state.

Introduction

We have previously reported that palladium bis(hexafluoroacetylacetonate), Pd(F$_6$acac)$_2$, behaves as a strong Lewis acid and forms an extensive series of crystalline complexes with molecular Lewis bases, L.[1,2] These can be grouped into four classes according to stoichiometry and have the general formula Pd(F$_6$acac)$_2$L$_n$, where n is 1, 2, 3, or 4. An investigation of the $n = 1$ class, along with an X-ray crystal structure of Pd(F$_6$acac)$_2$(CH$_3$)$_2$NH, showed that the 1:1 adducts contain four-coordinate palladium with one bidentate oxygen-bonded hexafluoroacetylacetonate ligand (F$_6$acac-*O,O*) and one carbon-bonded -CH(COCF$_3$)$_2$ group (F$_6$acac-*C*).[3] During the course of a systematic NMR study of the reactions of Pd(F$_6$acac)$_2$ with different Lewis bases, we found evidence for the presence of minor amounts of 1:1 complexes which had spectroscopic properties different from the previously characterized Pd(F$_6$acac-*O,O*)(F$_6$acac-*C*)L materials.[4] Compounds of this new isomeric class are formed in high yield with phosphine donors. This paper describes the preparation of adducts with phosphorus bases and the delineation by ^{19}F DNMR spectroscopy and X-ray crystallography of fluxional behavior in representative members of this class, Pd(F$_6$acac)$_2$PPh$_3$ and Pd(F$_6$acac)$_2$P(*o*-tolyl)$_3$.

Results

The reaction between Pd(F$_6$acac)$_2$ and triphenylphosphine in chloroform was monitored by ^{19}F NMR spectroscopy. Only 1 equiv of the phosphine is consumed and, when the P:Pd ratio is 1:1, Pd(F$_6$acac-*O,O*)(F$_6$acac-*C*)PPh$_3$, with $\delta(^{19}$F) 76.14 (1 F), 76.17 (1 F), and 76.30 (2 F) and $\delta(^{31}$P) 38.3, is produced along with the new isomeric compound Pd(F$_6$acac)$_2$PPh$_3$ (**1**). As will be shown below, **1** contains a monodentate oxygen-bonded F$_6$acac group and may be written as Pd(F$_6$acac-*O,O*)(F$_6$acac-*O*)PPh$_3$. The molar ratio of the carbon-bonded isomer to **1** is 0.2:1. Pure, crystalline samples of **1** may be obtained by cooling hexane solutions of Pd(F$_6$acac)$_2$ and triphenylphosphine. Titration experiments with tri-*o*-tolylphosphine showed that only Pd(F$_6$acac-*O,O*)(F$_6$acac-*O*)P(*o*-tolyl)$_3$ (**2**), with $\delta(^{19}$F) 76.22 and $\delta(^{31}$P) 19.4, is formed in chloroform. In methanol, complexation of an additional 1 mol of triphenylphosphine occurs to form Pd(F$_6$acac)$_2$(PPh$_3$)$_2$, a member of the 2:1 adduct class, which was isolated as the hexafluorophosphate salt [(Ph$_3$P)$_2$Pd(F$_6$acac)]PF$_6$ (**3**). The reaction of Pd(F$_6$acac)$_2$ with 3 equiv or more of triphenylphosphine in methanol led to reduction of the metal and the formation of Pd(PPh$_3$)$_4$. There is a parallel between the chemistry of triphenylphosphine and triphenylarsine with the important exception that, in chloroform, the ratio of Pd(F$_6$acac-*O,O*)(F$_6$acac-*C*)AsPh$_3$ to Pd(F$_6$acac-*O,O*)(F$_6$acac-*O*)AsPh$_3$ is substantially larger, 2.2:1.

---

* To whom correspondence should be addressed at the 3M Central Research Laboratory.

(1) A. R. Siedle, R. A. Newmark, and L. H. Pignolet, *J. Am. Chem. Soc.*, **103**, 4947 (1981).

(2) A. R. Siedle, R. A. Newmark, A. A. Kruger, and L. H. Pignolet, *Inorg. Chem.*, **20**, 3399 (1981).

(3) A. R. Siedle and L. H. Pignolet, *Inorg. Chem.*, **20**, 1849 (1981).

(4) A. R. Siedle, R. A. Newmark, and L. H. Pignolet, to be submitted for publication.

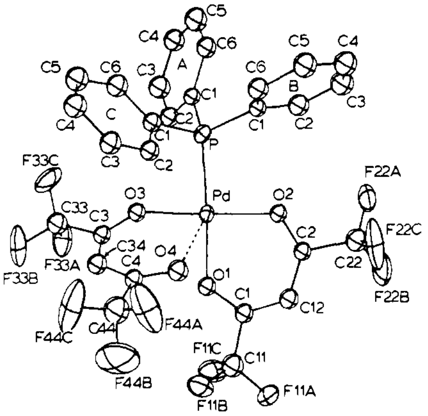

Figure 1. ORTEP drawing of $Pd(F_6acac)_2(PPh_3)$ showing the labeling scheme. The primed and unprimed molecules have identical labels except for the prime designator.

Bis(diphenylphosphino)acetylene yields $Pd(F_6acac\text{-}O,O)(F_6acac\text{-}O)Ph_2PC_2PPh_2$ (**4**), a 1:1 adduct in which only one phosphine is bonded to palladium. In contrast, the coordination chemistry of this acetylenic diphosphine with group 1B metals is more complex, and materials in which both phosphorus atoms act as donors may be isolated.[5]

Titration experiments were carried out in which ^{19}F NMR spectroscopy was used to follow the reactions of $Pd(F_6acac)_2$ with trimethyl phosphite in chloroform. When the phosphite:palladium ratio was 0.5:1, a peak at δ 75.82, attributed to $Pd(F_6acac\text{-}O,O)(F_6acac\text{-}O)P(OMe)_3$ was observed along with another at δ 76.91 due to $Pd(F_6acac)_2[P(OMe)_3]_2$ (**5**). As more trimethyl phosphite was added, the 76.91-ppm resonance sharpened and increased in intensity while those at δ 75.82 and 73.63 (unreacted $Pd(F_6acac)_2$) diminished. A pure sample of **5** was prepared by combining $Pd(F_6acac)_2$ with 2 equiv of trimethyl phosphite in pentane. It had $\delta(^{19}F)$ of 76.78, in good agreement with the chemical shifts observed in the titration experiments.

Similar titrations with the more basic triisopropyl phosphite indicated that only a 2:1 adduct with $\delta(^{19}F)$ 76.27 was formed in significant amounts.

In contrast to the chemistry observed with triphenylphosphine, reduction did not occur when $Pd(F_6acac)_2$ in methanol was treated with excess trimethyl phosphite or triethylphosphine. Rather, total displacement of the hexafluoroacetylacetonate ligands occurred and, after addition of ammonium hexafluorophosphate, the cationic palladium complexes $[(MeO)_3P]_4Pd(PF_6)_2$ (**6**) and $(Et_3P)_4Pd(PF_6)_6$ (**7**) were isolated in high yield. In agreement with other workers, we find that the ^{31}P NMR spectra of **6** and **7** are quite complicated due to ligand dissociation, exchange, and coupling phenomena.[6,7] Cyclopalladation reactions of ligands coordinated to $Pd(F_6acac)_2$ are known to be quite facile.[8] Triphenylphosphite was ortho metalated even at low temperatures to form $(PhO)_2POC_6H_4Pd(F_6acac)$ (**8**) and hexafluoroacetylacetone, so that the intermediate adduct could not be unambiguously identified. For a further characterization of the new class of 1:1 Lewis base adducts of $Pd(F_6acac)_2$, an X-ray crystal structure determination on **1** was undertaken.

Description of the Structure. The crystal structure of $Pd(F_6acac)_2(PPh_3)$ consists of well-separated molecular units. The shortest intermolecular contacts are 3.14 (1) Å for O2---F22C′ and 3.09 (1) Å for F11A---F44B′. The two independent molecules in the asymmetric unit are labeled with primed and unprimed names such that chemically equivalent atoms have the same designation except for the primes. Figures 1–3 show ORTEP drawings of the molecular structure of the unprimed molecule. There were no significant differences between the molecular structures of the two molecules. Selected distances and angles are presented in Table II and Figure 2. Since there are not significant differences in the distances and angles between the two molecules, averaged values are presented in Figure 2 and will be used in the following discussion.

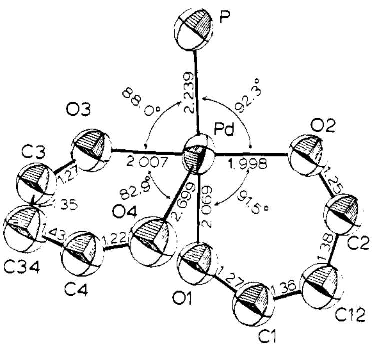

Figure 2. ORTEP drawing of the coordination core of $Pd(F_6acac)_2(PPh_3)$ with selected distances and angles. The values are averaged over the two independent molecules.

The geometry of the coordination core is best described as distorted square pyramidal with a weak axial interaction. The atoms comprising the square base (O1, O2, P, O3) are planar with a maximum deviation from their weighted least-squares plane (planes 1 and 3, Table S3 (supplementary material)) of 4 and 7 esd for the unprimed and primed molecules, respectively. The Pd atom is displaced 0.06 Å out of this plane in the direction of the axial oxygen atom O4. The major distortion from ideal square-pyramidal geometry is caused by the smaller than 90° "bite" angle of the semichelating F_6acac ligand (O_3–Pd–O_4, 82.9 (2)°) and steric repulsion between the atoms in phenyl ring C and O4. This latter interaction causes opening of the O4–Pd–P angle to 107.7 (2)° and closing of the O4–Pd–O1 angle to 73.7 (2)° compared with idealized values of 90°. The O4–Pd–O2 angle is 102.0 (2)°.

The basal bidentate F_6acac chelate ring is planar within experimental error (planes 3 and 4, Table S3). The Pd atom is displaced 0.22 Å out of this plane. The F_6acac semichelating ring, which spans basal and axial positions, is also planar within experimental error (planes 5 and 6, Table S3), and the Pd atom is displaced only 0.08 Å out of this plane. This semichelating ring (planes 5, Table S3) makes a dihedral angle of 72° with the plane formed by O1, O2, O3, and P atoms in the square base. The basal Pd–O distances which are mutually trans are identical (average 2.003 (5) Å) and are similar to values found in other $Pd(F_6acac)$ complexes where the oxygen is trans to either an oxygen[9] or nitrogen[3] atom. The basal Pd–O bond which is trans to the phosphine is longer (2.069 (5) Å) presumably due to the trans structural influence of phosphorus. The Pd–O distance to the axial O4, the other terminus of the semichelating F_6acac group, is quite long (2.699 (6) Å) and comparable to the 2.653 (6) Å distance in $(triphos)Pd(F_6acac)^{+}$[4] but notably shorter than the 3.1-Å distance observed in $[Pd(4\text{-}ClC_5H_4N)_4](F_6acac)_2$.[10] In a similar complex,[9] $Pd(F_6acac)_2P(o\text{-}tolyl)_3$ (**2**), which has the same overall geometry, the Pd–O axial distance is somewhat longer (2.797 (6) Å) presumably due to steric crowding of the o-tolyl groups. In this complex, the F_6acac ligand that spans the basal-axial positions is significantly folded whereas in the triphenylphosphine case the ligand is planar (vide supra). This folding is due to repulsion of an o-tolyl group.[9] The bonding within the F_6acac ligand in the basal plane of $Pd(F_6acac)_2(PPh_3)$ is symmetric whereas it is unsymmetric in the basal-axial spanning ligand (C3–O3, 1.27 (1); C4–O4, 1.22 (1); C34–C3, 1.35 (1), C34–C4, 1.43 (1) Å) and indicates a significant contribution from the resonance structure

$$\overline{\mathrm{Pd{-}O{-}C(CF_3){=}CH{-}C(CF_3){=}O}}$$

---

[5] A. J. Carty and A. Efraty, *Inorg. Chem.*, **8**, 543 (1969).

[6] D. A. Couch and S. D. Robinson, *J. Chem. Soc., Chem. Commun.*, 1508 (1971).

[7] P. Meakin and J. P. Jesson, *J. Am. Chem. Soc.*, **96**, 5751 (1974).

[8] A. R. Siedle, *J. Organomet. Chem.*, **208**, 115 (1981).

[9] S. Okeya, T. Miyamoto, S. Ooi, Y. Nakamura, and S. Kawaguchi, *Inorg. Chim. Acta*, **45**, L135 (1980).

[10] A. R. Siedle and L. H. Pignolet, *Inorg. Chem.*, **21**, 135 (1982).

Table I. Positional and Isotropic Thermal Parameters[a]

atom	x	y	z	B, Å^2	atom	x	y	z	B, Å^2
Pd	0.25828 (4)	0.34209 (5)	0.84515 (3)		C44	0.1313 (0)	0.5836 (0)	0.9509 (0)	0.2 (0)
Pd′	0.25223 (4)	0.13719 (5)	1.15617 (3)		C1A	0.3815 (5)	0.4003 (7)	0.7579 (4)	4.6 (2)
P	0.3543 (1)	0.4212 (2)	0.8301 (1)		C2A	0.3353 (6)	0.3812 (9)	0.7128 (5)	6.2 (3)
P′	0.3483 (1)	0.0580 (2)	1.1807 (1)		C3A	0.3565 (6)	0.3650 (9)	0.6581 (5)	6.9 (3)
F11A	0.0738 (4)	0.1009 (6)	0.9252 (5)		C5A	0.4608 (6)	0.3912 (10)	0.6913 (5)	7.5 (3)
F11B	0.0547 (4)	0.2578 (7)	0.9183 (4)		C6A	0.4485 (6)	0.4076 (9)	0.7483 (5)	6.9 (3)
F11C	0.0535 (4)	0.1687 (8)	0.8432 (5)		C1B	0.4261 (5)	0.3861 (7)	0.8764 (4)	4.3 (2)
F22A	0.3741 (4)	0.0975 (8)	0.9425 (5)		C2B	0.4448 (6)	0.2842 (9)	0.8766 (5)	6.3 (3)
F22B	0.2995 (6)	0.0049 (7)	0.9504 (5)		C3B	0.5027 (7)	0.2565 (11)	0.9120 (6)	8.3 (3)
F22C	0.3199 (5)	0.1084 (8)	1.0053 (3)		C4B	0.5382 (6)	0.3286 (10)	0.9453 (5)	7.4 (3)
F33A	0.1173 (5)	0.4916 (7)	0.7075 (3)		C5B	0.5195 (6)	0.4273 (10)	0.9431 (5)	6.8 (3)
F33B	0.1030 (6)	0.6291 (6)	0.7445 (3)		C6B	0.4624 (5)	0.4575 (8)	0.9082 (4)	5.6 (2)
F33C	0.1940 (5)	0.5875 (8)	0.7117 (3)		C1C	0.3429 (4)	0.5564 (7)	0.8382 (1)	4.1 (2)
F44A	0.1514 (5)	0.5711 (7)	1.0002 (3)		C2C	0.3218 (5)	0.5902 (8)	0.8905 (5)	5.7 (2)
F44B	0.1048 (6)	0.6688 (6)	0.9366 (4)		C3C	0.3106 (6)	0.6987 (9)	0.8987 (5)	6.5 (3)
F44C	0.0735 (0)	0.5500 (0)	0.9592 (0)		C4C	0.3213 (6)	0.7620 (9)	0.8521 (5)	6.2 (3)
F11A′	0.0704 (4)	0.3767 (6)	1.0527 (4)		C5C	0.3401 (6)	0.7293 (9)	0.8024 (5)	6.8 (3)
F11B′	0.0476 (3)	0.2237 (6)	1.0675 (4)		C6C	0.3521 (5)	0.6228 (9)	0.7938 (5)	5.9 (3)
F11C′	0.0503 (4)	0.3273 (7)	1.1342 (4)		C1′	0.1541 (5)	0.2789 (8)	1.1015 (4)	5.1 (2)
F22A′	0.3686 (4)	0.4017 (7)	1.0098 (4)		C2′	0.2675 (5)	0.3121 (7)	1.0846 (4)	4.5 (2)
F22B′	0.2921 (5)	0.4780 (6)	1.0521 (5)		C12′	0.2008 (5)	0.3318 (8)	1.0762 (4)	5.5 (2)
F22C′	0.3305 (5)	0.3611 (7)	1.0086 (4)		C11′	0.0030 (6)	0.3000 (10)	1.0068 (5)	7.3 (3)
F33A′	0.1142 (4)	−0.0150 (6)	1.2784 (3)		C22′	0.3158 (6)	0.3865 (10)	1.0586 (5)	7.1 (3)
F33B′	0.0961 (5)	−0.1513 (6)	1.2383 (3)		C3′	0.1643 (5)	−0.0317 (7)	1.1924 (4)	4.6 (2)
F33C′	0.1882 (4)	−0.1213 (7)	1.2758 (3)		C4′	0.1524 (5)	−0.0383 (7)	1.0858 (4)	4.6 (2)
F44A′	0.1507 (5)	−0.0972 (8)	0.9902 (4)		C34′	0.1388 (5)	−0.0699 (8)	1.1407 (4)	5.4 (2)
F44B′	0.0655 (6)	−0.0628 (11)	1.0203 (5)		C33′	0.1423 (6)	−0.0827 (9)	1.2467 (5)	6.4 (3)
F44C′	0.1037 (7)	−0.1878 (6)	1.0478 (4)		C44′	0.3770 (5)	−0.0793 (7)	1.2557 (4)	4.3 (2)
O1	0.1663 (3)	0.2735 (5)	0.8521 (3)	5.0 (1)	C2A′	0.3309 (5)	0.1002 (8)	1.2936 (4)	5.5 (2)
O2	0.3038 (3)	0.2356 (5)	0.8944 (3)	4.7 (1)	C3A′	0.3531 (6)	0.1126 (10)	1.3552 (5)	7.6 (3)
O3	0.2131 (3)	0.4419 (5)	0.7904 (3)	4.7 (1)	C4A′	0.4211 (6)	0.1072 (9)	1.3714 (5)	6.7 (3)
O4	0.1967 (3)	0.4515 (5)	0.9251 (3)	5.9 (2)	C5A′	0.4654 (6)	0.0842 (10)	1.3298 (5)	7.5 (3)
O1′	0.1613 (3)	0.2068 (5)	1.1385 (3)	4.9 (1)	C6A′	0.4445 (5)	0.0704 (9)	1.2711 (5)	5.8 (2)
O2′	0.2988 (3)	0.2448 (5)	1.1129 (3)	4.5 (1)	C18′	0.4169 (4)	0.0967 (7)	1.1395 (4)	4.3 (2)
O3′	0.2065 (3)	0.0385 (5)	1.2066 (3)	4.7 (1)	C28′	0.4402 (6)	0.1958 (9)	1.1453 (5)	6.3 (3)
O4′	0.1879 (3)	0.0307 (5)	1.0707 (3)	5.8 (2)	C3B′	0.4953 (6)	0.2260 (10)	1.1159 (5)	7.6 (3)
C1	0.1578 (5)	0.2054 (8)	0.8893 (4)	5.5 (2)	C4B′	0.5249 (6)	0.1572 (10)	1.0788 (5)	7.2 (3)
C2	0.2714 (5)	0.1705 (8)	0.9204 (4)	5.0 (2)	C5B′	0.5019 (6)	0.0619 (10)	1.0723 (5)	7.2 (3)
C12	0.2044 (6)	0.1500 (9)	0.9231 (5)	6.2 (3)	C6B′	0.4468 (5)	0.0272 (9)	1.1032 (5)	5.9 (3)
C11	0.0846 (7)	0.1799 (11)	0.8953 (6)	8.7 (4)	C1C′	0.3384 (5)	−0.0794 (8)	1.1707 (4)	4.7 (2)
C22	0.3172 (6)	0.0959 (10)	0.9551 (5)	7.7 (3)	C2C′	0.3135 (5)	−0.1135 (8)	1.1180 (4)	5.0 (2)
C3	0.1720 (5)	0.5106 (7)	0.7998 (4)	4.4 (2)	C3C′	0.3065 (6)	−0.2180 (9)	1.1082 (5)	6.2 (3)
C4	0.1612 (5)	0.5207 (8)	0.9062 (4)	5.1 (2)	C4C′	0.3251 (6)	−0.2837 (10)	1.1532 (5)	7.1 (3)
C34	0.1466 (5)	0.5524 (8)	0.8459 (4)	5.4 (2)	C5C′	0.3477 (6)	−0.2501 (10)	1.2081 (5)	7.3 (3)
C33	0.1481 (6)	0.5582 (10)	0.7424 (5)	7.0 (3)	C6C′	0.3575 (6)	−0.1430 (9)	1.2188 (5)	6.6 (3)

[a] ESD's of the last figures are in parentheses. Anisotropic thermal parameters are available as supplementary material.

Table II. Selected Distances and Angles in $Pd(F_6acac)_2(PPh_3)$

				Distances, Å[a]				
Pd-P	2.240 (3)	2.237 (3)	C1-C12	1.39 (1)	1.33 (1)	C11-F11C	1.33 (2)	1.36 (2)
Pd-O1	2.074 (5)	2.064 (5)	C1-C11	1.53 (1)	1.48 (1)	C22-F22A	1.20 (2)	1.26 (2)
Pd-O2	1.994 (5)	2.001 (5)	C2-C12	1.38 (1)	1.37 (1)	C22-F22B	1.25 (2)	1.30 (2)
Pd-O3	2.005 (5)	2.008 (5)	C2-C22	1.54 (1)	1.53 (1)	C22-F22C	1.18 (2)	1.26 (2)
Pd-O4	2.706 (6)	2.691 (6)	C3-C34	1.33 (1)	1.37 (1)	C33-F33A	1.32 (2)	1.30 (2)
P-C1A	1.813 (9)	1.819 (8)	C3-C33	1.52 (1)	1.52 (1)	C33-F33B	1.30 (2)	1.30 (2)
P-C1B	1.805 (8)	1.800 (8)	C4-C34	1.47 (1)	1.38 (1)	C33-F33C	1.26 (2)	1.22 (2)
P-C1C	1.805 (8)	1.833 (9)	C4-C44	1.48 (1)	1.49 (1)	C44-F44A	1.21 (2)	1.29 (2)
O1-C1	1.262 (10)	1.281 (9)	C11-F11A	1.28 (2)	1.30 (2)	C44-F44B	1.25 (2)	1.25 (2)
O2-C2	1.253 (9)	1.249 (9)	C11-F11B	1.32 (2)	1.29 (2)	C44-F44C	1.30 (2)	1.23 (2)
O3-C3	1.253 (9)	1.284 (9)						
O4-C4	1.222 (9)	1.219 (9)						
				Angles, Deg[a]				
O1-Pd-O2	91.7 (2)	91.3 (2)	Pd-P-C1A	112.6 (2)	113.0 (3)	O3-C3-C34	137 (1)	134 (1)
O3-Pd-O4	82.9 (2)	82.9 (2)	Pd-P-C1B	117.2 (3)	114.3 (3)	O3-C3-C33	109 (1)	109 (1)
P-Pd-O1	175.0 (2)	176.3 (2)	Pd-P-C1C	109.0 (2)	110.0 (2)	O4-C4-C34	129 (1)	130 (1)
P-Pd-O2	92.7 (2)	91.9 (2)	Pd-O1-C1	121.4 (5)	121.6 (5)	O4-C4-C44	115 (1)	115 (1)
P-Pd-O3	87.6 (2)	88.3 (2)	Pd-O2-C2	121.5 (5)	121.9 (5)	C1-C12-C2	120 (1)	123 (1)
P-Pd-O4	107.1 (2)	108.2 (2)	Pd-O3-C3	129.8 (5)	129.4 (4)	C3-C34-C4	126 (1)	128 (1)
O4-Pd-O1	74.4 (2)	72.9 (2)	Pd-O4-C4	115.7 (5)	116.1 (5)	C1-C11-F11[b]	111 (1)	115 (1)
O4-Pd-O2	101.3 (2)	102.6 (2)	O1-C1-C12	130 (1)	129 (1)	C2-C22-F22[b]	114 (1)	114 (1)
O1-Pd-O3	87.9 (2)	88.3 (2)	O1-C1-C11	113 (1)	111 (1)	C3-C33-F33[b]	114 (1)	112 (1)
O2-Pd-O3	175.5 (2)	174.2 (2)	O2-C2-C12	134 (1)	132 (1)	C4-C44-F44[b]	115 (1)	115 (1)
			O2-C2-C22	112 (1)	110 (1)			

[a] Values given for unprimed and primed atoms, respectively. [b] Values are averaged over three equivalent angles to FA, FB and FC.

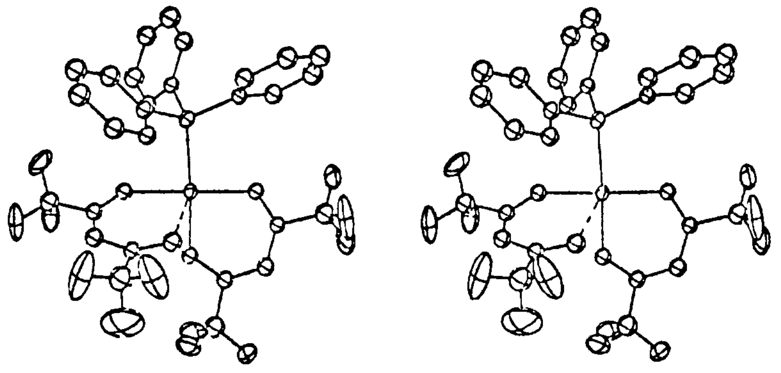

Figure 3. ORTEP stereoview of $Pd(F_6acac)_2(PPh_3)$ (unprimed molecule shown).

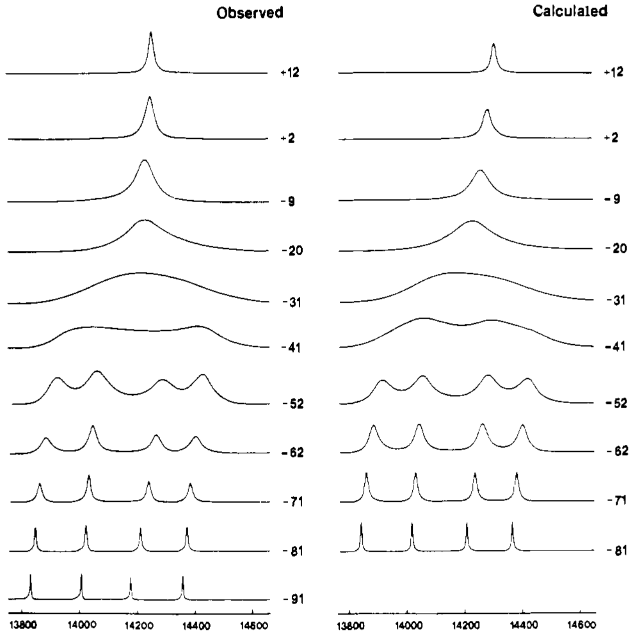

Figure 4. Calculated and observed ^{19}F DNMR spectra of $Pd(F_6acac)_2P(o\text{-tolyl})_3$ (**2**).

Table III. Exchange-Corrected Chemical Shifts of $(o\text{-tolyl})_3PPd(F_6acac)_2$ (2) at Low Temperatures[a]

temp, °C	ν_A	ν_B	ν_C	ν_D
−91	13 831	14 007	14 177	14 357
−81	13 847	14 021	14 209	14 370
−71	13 861	14 033	14 240	14 384
−62	13 882	14 046	14 265	14 404
−52	13 912	14 060	14 287	14 436

[a] In Hz from $CFCl_3$ at 188.2 MHz.

Such unsymmetrical bonding has been observed in $Pd(F_6acac)_2P(o\text{-tolyl})_3$ and in $Pd(F_6acac)_2[(CH_3)_2NH]$.[3] The Pd–P distance (2.239 (3) Å) is similar to values observed in other PPh_3 complexes of palladium.[11]

Solution-Phase Properties. Complexes of the type $Pd(F_6acac\text{-}O,O)(F_6acac\text{-}C)L$ are characterized by two singlets of area 1 in their ^{19}F NMR spectra due to the nonequivalent CF_3 groups in the $F_6acac\text{-}O,O$ ligand and a singlet of relative area 2 due to the $-CH(COCF_3)_2$ trifluoromethyl groups. In addition, the uncoordinated $COCF_3$ moieties give rise to a strong carbonyl absorption at about 1730 cm^{-1} in the infrared spectra.[3] In contrast, $Pd(F_6acac\text{-}O,O)(F_6acac\text{-}O)PPh_3$ and other members of this new class of 1:1 $Pd(F_6acac)_2$ complexes reported here do not show carbonyl type infrared absorptions, either in solution or as Nujol mulls. In addition, their ^{19}F NMR spectra at room temperature comprise one singlet resonance even in the presence of a large excess of the phosphine donor. This requires operation of a dynamic process, rapid on the NMR time scale, which interconverts the CF_3 groups in the $F_6acac\text{-}O,O$ and $F_6acac\text{-}O$ ligands. Low-temperature ^{19}F NMR spectra were obtained on **1**, but no evidence of dynamic equilibria was observed above −80 °C, at which temperature the compound precipitated from the methylene chloride solution.

Spectra of $(o\text{-tolyl})_3PPd(F_6acac)_2$ (**2**) show four sharp peaks of equal area at low temperature at 73.48, 74.41, 75.31, and 76.27 ppm (see Figure 4) due to the four inequivalent perfluoromethyl groups in the molecule. These four peaks coalesce at ca. −40 °C due to a dynamic equilibrium involving the two F_6acac ligands. At temperatures below coalescence, all four peaks show line widths that are the same within experimental error, indicating that exchange with respect to any site is equally probable. Consequently, equations representing the dynamic equilibria were analyzed in which equal exchange rates between all four perfluoromethyl absorptions were assumed. The calculation, based on the exchange-modified classical Bloch equations,[12] is described in the appendix (supplementary material). The good fit between the observed and calculated spectra confirms the assumption that the dynamic equilibria involve a symmetrical transition state in which exchange between all four sites is equally probable (cf. Figure 4).

Spectra were fit at low temperatures (−91 to −52 °C) to the average line widths and frequencies of the four absorptions. At low temperatures (see Table III) peaks A, B, and D show a small (1.5 Hz/deg) variation with temperature, but peak C shifts at a 2-fold faster rate, suggesting C should be assigned to the unique CF_3 group attached to C4. As exchange becomes faster and the peaks broaden, a nonlinear shift of the frequencies becomes apparent. In particular, peak D shows increasingly large upfield shifts with temperature. The chemical shifts in Table III are the true chemical shifts of the peaks after correcting for frequency shifts due to the dynamic equilibria. These corrections are 2 Hz at −62 °C and 11 Hz at −52 °C for peaks A and D. Since the calculated chemical shifts depend on the exchange pathway, other mechanisms were considered to see if they would result in a more linear temperature dependence of the chemical shifts. Exchange between pairs of CF_3 sites at equal rates could be invoked to calculate the chemical shifts. Spectra were calculated with the assumption of a standard two-site exchange process and the exchange-corrected chemical shifts of the exchange broadened peaks determined. These chemical shifts were considerably more nonlinear vs. temperature than those given in Table III, especially for peak D. Since the spectrum at −31 °C shows a single broad resonance, it was required that the equilibrium between the two pairs of F_6acac ligands become rapid by −31 °C in any case. Thus, the dynamic NMR spectra are strongly indicative of equal lifetimes for all CF_3 sites.

The chemical shifts relative to reference $CFCl_3$ at −91, −81, −71, −62, and −52 °C were then extrapolated to higher temper-

---

(11) G. J. Palenik, M. Mathew, W. L. Steffen, and G. Beran, *J. Am. Chem. Soc.*, **97**, 1059 (1975).

(12) G. Binsch, *Top. Stereochem.*, **3**, 97 (1968); D. S. Thompson, R. A. Newmark, and C. H. Sederholm, *J. Chem. Phys.*, **37**, 411 (1962); R. A. Newmark, Thesis, University of California, Berkeley, CA, 1964.

Table IV. Lifetimes $\tau = 1/k$ and Free Energies of Activation for $(o\text{-tolyl})_3PPd(F_6acac)_2$ (2)

temp, °C	τ	$\Delta G^{\ddagger}$	temp, °C	τ	$\Delta G^{\ddagger}$
−81	2.23	11.37	−31	0.044	12.58
−71	0.91	11.62	−20	0.019	12.76
−62	0.38	11.83	−9	0.0085	12.90
−52	0.19	12.11	+2	0.0041	13.04
−41	0.076	12.27	+12	0.0021	13.19

atures with use of a parabolic fit to inverse temperature. The fit between the averaged chemical shifts of the four peaks and the observed apparent shift is in error by 37 Hz at −9 °C and 55 Hz at +12 °C. Both calculated and observed spectra indicate a significant upfield shift of the coalesced peak at high temperatures, but the calculated rate of 2.3 Hz/deg exceeds the observed rate of 1.5 Hz/deg. Thus, the rates at higher temperature may be in error. Since the extrapolated values of peak D appeared most likely to be incorrect, spectra were calculated with ±100-Hz variations in τ at +12 °C. These calculations showed the error in τ would be under 25% for this change in the chemical shift, which would affect $\Delta G^{\ddagger}$ by 0.18 kcal/mol.

Optimum values of τ that best fit the observed spectra are given in Table IV. Free energies of activation were calculated from absolute reaction rate theory:

$$\frac{1}{\tau} = \frac{kT}{h} e^{-\Delta G^{\ddagger}/RT}$$

The temperature dependence of $\Delta G^{\ddagger}$ yields $\Delta H^{\ddagger} = 7.7$ kcal/mol and $\Delta S^{\ddagger} = -20$ eu. The major errors in this expression are the systematic errors in the temperature, which affect the calculation of $\Delta G^{\ddagger}$ given in Table IV, and the error in the extrapolated chemical shifts, which affects the high-temperature rates. Assuming maximum errors of ±2 °C in the lower temperatures, ∓2 °C in the upper temperatures, and 25% in the high-temperature rate gives errors of ±1.0 kcal/mol in $\Delta H^{\ddagger}$ and ±5 eu in $\Delta S^{\ddagger}$. The errors are relatively small for NMR rate studies because of the large temperature range over which coalescence of the peaks is observed due to the considerable chemical shift differences between the four resonances.

Discussion

Displacement of both hexafluoroacetylacetonate ligands from $Pd(F_6acac)_2$ by trimethyl phosphite or triethylphosphine is facile, but triarylphosphines form a new isomeric class of 1:1 adducts. These compounds contain a semichelating F_6acac ligand attached to the metal by a normal Pd–O bond but which is oriented so that the remaining oxygen terminus forms a long metal–oxygen contact. This type of bonding for a β-diketonate was first observed by us in $(triphos)Pd(F_6acac)^+$.[1] Members of this class are stereochemically nonrigid in solution. One of the most striking features of the ^{19}F DNMR spectra of $Pd(F_6acac)_2P(o\text{-tolyl})_3$ is the simultaneous coalescence of all four singlet resonances. This result implies that the molecule passes through a highly symmetrical transition state in which all four CF_3 groups are equivalent. Complete cleavage of the Pd–P bond is probably not involved in the fluxional process since ^{19}F NMR spectra show that Ph_3P does not exchange rapidly on the NMR time scale between $Pd(F_6acac)_2PPh_3$ and $Pd(F_6acac)_2$ at room temperature. Similarly, separate ^{19}F resonances were observed for a mixture of **1** and **2** in chloroform at room temperature, indicating that rapid intermolecular F_6acac exchange does not occur.

The thermodynamic parameters for F_6acac rearrangement in **2** are $\Delta H^{\ddagger} = 7.7 \pm 1$ kcal/mol and $\Delta S^{\ddagger} = -20 \pm 5$ eu. These values are quite similar to those found for the intramolecular rearrangement of the semichelating F_6acac group in $(triphos)Pd(F_6acac)^+BPh_4^-$, for which $\Delta H^{\ddagger}$ is 8.1 ± 1 kcal/mol and $\Delta S^{\ddagger}$ is -21 ± 3 eu.[1] The barrier to rearrangement in $Pd(F_6acac)_2P(aryl)_3$ is a sensitive function of the steric properties of the aryl group. If we assume that the ^{19}F chemical shifts in the limiting low-temperature spectra of **1** and **2** are the same, then the activation energies for permutation of the CF_3 groups in **1** are at least 2.5 kcal/mol lower.

Thus, the barrier to rearrangement in $Pd(F_6acac)_2P(aryl)_3$ is a function of the steric properties of the aryl group and increases as the size of $P(aryl)_3$ increases. This process may involve the formation of a trigonal-bipyramidal intermediate which undergoes a Berry twist rapidly on the NMR time scale. An attractive and plausible alternative structure for the transition state, related by the principle of microscopic reversibility to the starting materials is a C_{2v} square-based pyramidal structure with two bidentate planar, basal F_6acac groups and an apical phosphine. In this model transition state, in which all four CF_3 groups are equivalent, it is reasonable to suppose that the apical Pd–O contact will be shorter than in the ground state and that the difference in steric strain associated with the different phosphine ligands makes a significant contribution to $\Delta H^{\ddagger}$ for the rearrangement. One anticipates that relief of strain caused by nonbonded repulsions would be associated with molecular distortion comparable to that produced by progress along the reaction coordinate leading to rearrangement.[13] Consistent with this thesis is the finding that, in going from $(o\text{-tolyl})_3P$ to Ph_3P in $Pd(F_6acac)_2P(aryl)_3$, there is indeed a 0.098-Å contraction in $d(Pd–O_{apical})$ (O4 in Figure 2) and a pronounced decrease in folding about the Pd–C34 vector of the semichelating F_6acac ligand. We note that fluxional behavior in the related $Ni(SacSac)(PEt_3)Cl$ has been described by Fackler and Masters.[14]

Experimental Section

Palladium bis(hexafluoroacetylacetonate) was prepared from $Na(F_6acac)$ and Na_2PdCl_4 in water as previously described.[2] ^1H and ^{19}F NMR spectra were obtained at 100 and 94.2 MHz, respectively, on a Varian XL-100 spectrometer. The ^{31}P spectra were obtained with square-wave proton decoupling on a Varian XL-200 spectrometer. Internal $(CH_3)_4Si$ and $CFCl_3$ and external 85% H_3PO_4 were used as references. Positive chemical shifts are downfield for the ^1H and ^{31}P shifts but upfield for ^{19}F. Infrared spectra were recorded on an instrument with grating optics and are believed to have an accuracy of ±5 cm^{-1}.

The ^{19}F DNMR spectra were obtained on a Varian XL-200 NMR spectrometer operating at 188.3 MHz. The sample was a 10% solution in CD_2Cl_2 containing $CFCl_3$ reference. Temperatures were determined with the Varian temperature controller. The latter was calibrated by using the neat methanol standard immediately after the analytical sample spectra were obtained. The temperature was then determined from the equations of Van Geet.[15] The consistency of the temperature calibration was confirmed by the smooth variation of the $CFCl_3$ chemical shift relative to the deuterium lock, which varied approximately 0.004 ppm (0.8 Hz)/deg. Sample spectra were obtained by averaging eight transients, with use of 2.0-s acquisition times, 30° (4 μs) RF pulses, a 2.8-s repetition rate, and 2000-Hz sweep widths. Only four transients were accumulated for the $CFCl_3$ peak. Spectra of the sample and reference regions were obtained consecutively in a 45-s time frame after allowing 7 min for thermal equilibrium at each temperature.

Spectra were calculated on an Apple II(+) microcomputer with disk and printer accessories by using the equations developed in the appendix. Spectra were first calculated at low temperatures where the four peaks were observable (−91 to −52 °C). These spectra were fit to the line width and observed peak frequency by systematically varying both the lifetime in a site and the site chemical shift. The true chemical shifts, after correction for the exchange at −62 and −52 °C, are given in Table III. The exchange rate at −41 °C was determined by a visual fit to the calculated spectra. At higher temperatures the exchange rate was systematically varied to fit the observed line width. The line width in the absence of exchange, taken as that of the reference $CFCl_3$, was under 3 Hz in all the DNMR spectra. This was subtracted from the observed line width to give the exchange broadening. This correction was not a significant factor due to the broad lines observed in the sample over the −81 to +12 °C range. Line shapes in CCl_4 were very similar to those in CD_2Cl_2.

$Pd(F_6acac)_2PPh_3$ (1). Triphenylphosphine (0.26 g, 1 mmol) and $Pd(F_6acac)_2$ (0.52 g, 1 mmol) were combined in 20 mL of warm hexane. The orange solution was concentrated and cooled to give 0.6 g of crude product. Two recrystallizations from pentane afforded 0.4 g (51%) of **1** as orange needles, mp 95 °C. Anal. Calcd: C, 43.1; H, 2.0. mol. wt.

---

(13) E. L. Muetterties, *Tetrahedron*, **30**, 1595 (1974); H. B. Burgi, *Inorg. Chem.*, **12**, 2331 (1973).

(14) J. P. Fackler, Jr., and R. F. Masters, *Inorg. Chim. Acta*, **39**, 111 (1980). SacSac is pentane-2,4-dithionato(1−).

(15) A. L. Van Geet, *Anal. Chem.*, **40**, 2227 (1968); **42**, 679 (1970); D. S. Raiford, C. L. Fisk, and E. D. Becker, *ibid.*, **51**, 2050 (1979).

782. Found: C, 43.1; H, 2.0. Molecular weight: calculated, 782; found (vapor pressure osmometry in $CHCl_3$), 739. NMR ($CDCl_3$; ppm, J in Hz): ^1H, 7.3–7.8 (m, 15 H), 5.82 (s, 2 H); ^{13}C, 174.2 (–C=O, $^2J_{CF}$ = 32), 118.6 (CF_3, J_{CF} = 285), 89.6 (methine CH, J_{CH} = 165); ^{19}F, 76.5 (s); ^{31}P, 20.9. IR (Nujol): 3060 (w), 1690 (s), 1630 (s), 1610 (s), 1560 (s), 1530 (m), 1480 (s), 1455 (s), 1430 (m), 1345 (m), 1260 (s), 1225 (m), 1200 (s), 1150 (s), 1100 (s), 1060 (m), 810 (m), 800 (m), 745 (m), 715 (m), 690 (s), 675 (m), 535 (s), 510 (m) cm^{-1}. Electronic spectrum ($CHCl_3$) (λ_{max}, log ϵ): 296 nm (4.19). $Pd(F_6acac)_2P(o\text{-tolyl})_3$ (**2**) was similarly prepared by combining equivalent amounts of $Pd(F_6acac)_2$ and tri-*o*-tolylphosphine; $\delta(^{19}F)$ = 76.16.

$[(Ph_3P)_2Pd(F_6acac)]PF_6$ (3). Triphenylphosphine (2.1 g, 8 mmol) and $Pd(F_6acac)_2$ (2.08 g, 4 mmol) were combined in 100 mL of methanol and stirred until the phosphine dissolved. After addition of excess methanolic NH_4PF_6, the reaction mixture was diluted to the cloud point with water and concentrated without heating on a rotary evaporator to give the yellow crystalline product. It was collected on a filter and washed with ether and then water. After vacuum drying, the yield was 3.7 g (94%). Anal. Calcd: C, 50.1; H, 3.2. Found: C, 49.7; H, 3.2. NMR (acetone; ppm, J in Hz): ^1H, 7.9–7.5 (m, 30 H), 6.30 (s, 1 H), ^{19}F, 71.7 (PF_6, J_{PF} = 708), 74.70 (CF_3, s); ^{31}P, –37.4 (s), –143.8 (h, J_{PF} = 707). IR(Nujol): 1640 (s), 1545 (m), 1450 (s), 1255 (s), 1210 (s), 1155 (s), 1105 (s), 1095 (s), 835 (s), 790 (m), 740 (m), 635 (m), 520 (m) cm^{-1}. Electronic spectrum (CH_3CN): 290 (ϵ 4.81), 350 (4.33) nm.

$Pd(F_6acac)_2(Ph_2PC_2PPh_2)$ (4). A solution of 0.39 g, 1 mmol, of 1,2-bis(diphenylphosphino)acetylene in 5 mL of benzene was added dropwise with stirring to 0.52 g, 1 mmol, of $Pd(F_6acac)_2$ in 3 mL of benzene. The orange flakes that separated were collected on a filter, washed with a small amount of fresh solvent, and then dried under vacuum. The yield was 0.39 g, 41%. Anal. Calcd: C, 46.1; H, 2.3; P, 6.6. Found: C, 46.2; H, 2.3; P, 7.0. NMR ($CDCl_3$; ppm): ^1H, 7.9–7.2 (m, 10 H), 5.95 (s, 1 H); ^{19}F, 76.6. IR (Nujol): 3060 (w), 1680 (s), 1550 (s), 1520 (m), 1480 (s), 1440 (s), 1380 (w), 1260 (s), 1205 (s), 1140 (s), 1070 (s), 1000 (w), 860 (s), 824 (m), 790 (m), 740 (m), 685 (s), 660 (s), 510 (s) cm^{-1}.

$Pd(F_6acac)_2[(MeO)_3P]_2$ (5). Trimethyl phosphite (0.50 g, 4 mmol) in 1 mL of pentane was added dropwise to 1.04 g (2 mmol) of $Pd(F_6acac)_2$ in 10 mL of pentane. The 2:1 adduct **5** separated as granular yellow solids, which were collected on a filter, washed with cold pentane, and briefly vacuum dried. The yield was 0.90 g (63%); mp 68 °C. A second crop of 0.20 g was obtained by cooling the filtrate to –78 °C. This compound appeared to decompose on standing and was stored under nitrogen in a refrigerator. Anal. Calcd: C, 25.0; H, 2.6. Found: C, 24.5; H, 2.7. The ^1H NMR spectrum in $CDCl_3$ showed a broad singlet at 4.0 ppm and a $P\text{–}OCH_3$ doublet (J = 12 Hz) at 3.77 ppm, indicating dissociation and/or decomposition of the compound. IR (Nujol): 1670 (s), 1640 (m), 1535 (s), 1255 (s), 1200 (s), 1150 (s), 1120 (s), 1030 (s), 815 (s), 795 (m), 770 (s), 750 (s), 660 (s), 575 (m), 530 (m) cm^{-1}.

$[(MeO)_3P]_4Pd(PF_6)_2$ (6). Trimethyl phosphite (1.24 g, 10 mmol) in 10 mL of methanol was added to 0.52 g, 1 mmol, of $Pd(F_6acac)_2$ in 5 mL of the same solvent. During the addition, the color of the reaction mixture turned from orange to pale yellow. Addition of excess methanolic NH_4PF_6 caused a white solid to separate. This was collected on a filter and recrystallized from acetone-ether containing 0.1 mL of trimethyl phosphite to afford 0.85 g (95%) of **6** as glistening white flakes. Anal. Calcd: C, 16.1; H, 4.2. Found: C, 15.9; H, 4.1. IR (Nujol): 1185 (s), 1060 (s), 1020 (s), 840 (s), 745 (s), 555 (s), 530 (s), 395 (w) cm^{-1}.

$(Et_3P)_4Pd(PF_6)_2$ (7). A solution of 0.52 g (1 mmol) of $Pd(F_6acac)_2$ in 25 mL of methanol was treated with excess triethylphosphine (67% solution in isopropanol, Aldrich Chemical Co.). Excess methanolic NH_4PF_6 was added, and the mixture was diluted to the cloud point with water. Slow concentration without heating on the rotary evaporator yielded 0.74 g (85%) of product as a bright yellow crystalline solid, which was collected on a filter, washed with water, and vacuum dried. Anal. Calcd: C, 33.1; H, 7.3. Found: C, 32.7; H, 7.1. IR (Nujol): 1035 (m), 875 (m), 840 (s), 770 (w), 755 (w), 555 (s) cm^{-1}. Electronic spectrum (CH_3CN): 222 (ϵ 2.39), 261 (2.09) nm.

$(PhO)_2POC_6H_4Pd(F_6acac)$ (8). A solution of 0.52 g, 1 mmol, of $Pd(F_6acac)_2$ and 0.31 g, 1 mmol, of triphenyl phosphite in 25 mL of hexane was refluxed for 1 h and then cooled in an ice bath. Filtration gave 0.20 g of white crystalline **8**, mp 98 °C. An additional 0.24 g was obtained by chromatography of the filtrate on silica gel with 1:1 benzene–hexane as the eluant. The total yield was 0.44 g (71%). Anal. Calcd: C, 44.4; H, 2.4. Found: C, 44.6; H, 2.1. NMR ($CDCl_3$; ppm): ^1H, 7.7–7.3 (m, 14 H), 6.12 (s, 1 H); ^{19}F, 76.09 (s); ^{31}P, –5.4 (s). IR (Nujol): 1640 (s), 1610 (w), 1560 (w), 1490 (s), 1460 (s), 1455 (s), 1255 (s), 1220 (s), 1210 (m), 1180 (s), 1155 (s), 1025 (m), 970 (s), 945 (s), 840 (s), 805 (m), 785 (m), 760 (m), 685 (m), 680 (m), 500 (m) cm^{-1}. Mass spectrum: m/e 622 (P^+).

Structure Determination. A crystal of $Pd(F_6acac)_2(PPh_3)$, $PdPF_{12}O_4C_{28}H_{17}$ (formula weight 782.8), of approximate dimensions 0.30 × 0.25 × 0.20 mm was selected and used in the structure determination. The crystal was found to belong to the monoclinic crystal class by the Enraf-Nonius CAD4-SDP peak searching, centering, and indexing computer programs.[16] The space group $P2_1/n$ was chosen from the systematic absences observed during data collection ($h0l$, $h + l = 2n + 1$; $0k0$, $k = 2n + 1$) and was verified by successful solution and refinement (vide infra). The unit cell dimensions were determined by least-squares refinement of the angular settings of 25 Mo $K\alpha$ (λ = 0.71069 Å) peaks centered on the diffractometer and are a = 20.106 (3) Å, b = 13.160 (7) Å, c = 23.185 (3) Å, β = 93.52 (3)°, and V = 6123 (5) Å^3. The density was calculated to be 1.698 g/cm^3 by using $Z = 8$.

Data collection was carried out using a CAD4 Nonius automatic diffractometer. A total of 10771 unique reflections were measured in the scan range 2θ = 0–50° over one quadrant ($+h,+k,+l$) with use of graphite-monochromatized Mo $K\alpha$ radiation and employment of a variable-rate ω-scan technique. No decay was noted in the intensity of 3 check reflections measured at intervals of 200 sequential reflections. Background counts were measured at both ends of the scan range with the scan equal, at each side, to one-fourth of the scan range of the peak. In this manner, the total duration of measuring backgrounds is equal to half of the time required for the peak scan. After correction for Lorentz, polarization, and background effects (but not for absorption; μ = 7.64 cm^{-1}),[17] 6536 reflections were judged observed ($F_o^2 \geq 2.0\sigma(F_o^2)$) and were used in all subsequent calculations.

Conventional heavy-atom techniques (Patterson synthesis) were used to locate the positions of two Pd atoms. Subsequent difference Fourier and least-squares calculations revealed the positions of all other nonhydrogen positions. Two entire $Pd(F_6acac)_2(PPh_3)$ molecules unrelated by symmetry within the $P2_1/n$ space group were found. Careful examination of the packing (long-range environment) around several chemically equivalent atoms of the two independent molecules eliminated the possibility of higher order symmetry. Therefore, refinement was carried out in the space group $P2_1/n$ with two molecules in the asymmetric unit.

Refinement with the palladium and fluorine atoms thermally anisotropic and all other non-hydrogen atoms thermally isotropic by full-matrix least-squares methods (509 variables) led to convergence of R and R_w to their final values of 0.071 and 0.086, respectively.[18] The error in an observation of unit weight was determined to be 2.38 by using a value

---

(16) All calculations were carried out on a PDP 11/34 computer using the Enraf-Nonius SDP programs. This crystallographic computing package is described by B. A. Frenz in "Computing in Crystallography", H. Schenk, R. Olthof-Hazekamp, H. van Koningsveld, and G. C. Bassi, Eds., Delft University Press, Delft, The Netherlands, 1978, pp 64–71.

(17) The intensity data were processed as described in "CAD4 and SDP Users Manual", Enraf-Nonius, Delft, The Netherlands, 1978. The net intensity I is given as

$$I = \frac{K}{\mathrm{NPI}}(C - 2B)$$

where K = 20.1166 times the attenuator factor, NPI = ratio of fastest possible scan rate to scan rate for the measurement, C = total count, and B = total background count. The standard deviation in the net intensity is given by

$$\sigma^2(I) = \left(\frac{K}{\mathrm{NPI}}\right)^2[C + 4B + (pI)^2]$$

where p is a factor used to downweight intense reflections. The observed structure factor amplitude F_o is given by

$$F_o = (I/Lp)^{1/2}$$

where Lp = Lorentz and polarization factors. The $\sigma(I)$'s were converted to the estimated errors in the relative structure factors $\sigma(F_o)$ by

$$\sigma(F_o) = \tfrac{1}{2}\frac{\sigma(I)}{I}F_o$$

(18) The function minimized was $\sum w(|F_o| - |F_c|)^2$, where $\omega = 1/\sigma^2(F_o)$. The unweighted and weighted residuals are defined as

$$R = (\sum||F_o| - |F_c||)/\sum|F_o| \qquad R_w = [(\sum w(|F_o| - |F_c|))^2/(\sum w|F_o|)^2]^{1/2}$$

The error in an observation of unit weight is

$$[\sum w(|F_o| - |F_c|)^2/(\mathrm{NO} - \mathrm{NV})]^{1/2}$$

where NO and NV are the number of observations and variables, respectively. Atomic scattering factors were taken from "International Tables for X-Ray Crystallography", Vol. III, Kynoch Press, Birmingham, England, 1962. Anomalous dispersion corrections from the same source were used for all non-hydrogen atoms.

of 0.04 for p in the $\sigma(I)$ equation.[17] The final difference Fourier map did not reveal any chemically significant features. The CF_3 groups show some signs of minor disorder, but simple disorder models did not improve the structure. In light of the goals of the structure determination, this point was not further pursued.

The final atomic coordinates with their estimated standard deviations and the final thermal parameters are given in Table I. Note that the chemically equivalent atoms of the two independent $Pd(F_6acac)_2(PPh_3)$ molecules are labeled with unprimed and primed names. Tables of observed and calculated structure factor amplitudes are available as supplementary material. Figure 1 presents an ORTEP perspective of the molecular structure of the unprimed $Pd(F_6acac)_2(PPh_3)$ molecule and shows the labeling scheme. The labeling scheme for the primed molecule is identical.

Registry No. 1, 83220-99-9; **2**, 75810-99-0; **3**, 83221-01-6; **4**, 83221-02-7; **5**, 83221-03-8; **6**, 83221-04-9; **7**, 83221-06-1; **8**, 83221-07-2.

Supplementary Material Available: Listings of observed and calculated structure factor amplitudes (Table S1), anisotropic thermal parameters (Table S2), and least-squares planes (Table S3) and an appendix containing a theoretical analysis of the DNMR spectra (34 pages). Ordering information is given on any current masthead page.

Surface-Modified Photochemistry. Preparation of Silica-Supported $Fe_3(CO)_{12}$ via Irradiation of Adsorbed $Fe(CO)_5$

Robert L. Jackson* and Mark R. Trusheim

Contribution from the Corporate Research Center, Allied Corporation, Morristown, New Jersey 07960. *Received December 18, 1981*

Abstract: The photochemistry of silica-adsorbed $Fe(CO)_5$ has been studied. IR and UV–visible spectra show that the only significant product is $Fe_3(CO)_{12}$ rather than $Fe_2(CO)_9$, which is the product observed following irradiation of $Fe(CO)_5$ in the gas or liquid phase or in solution. Formation of $Fe_3(CO)_{12}$ is discussed in terms of a mechanism involving rapid secondary thermal reactions of a surface-complexed form of $Fe(CO)_4$.

Introduction

Research in transition-metal catalysis has increasingly turned toward catalyst systems based on metal carbonyl complexes and their derivatives. These systems have led to significant technological advances, as metal carbonyls have directly or indirectly provided active catalysts for a number of important processes.[1] While most of these processes are catalyzed homogeneously, metal carbonyl complexes have recently been used as precursors in the synthesis of supported heterogeneous catalysts.[2-7] This technique has a number of advantages over more conventional methods proceeding via the reduction of supported metal salts. Catalyst preparation can be simplified, since metal carbonyls are often sufficiently volatile to allow their deposition directly onto the support from the gas phase. Supported metal carbonyls can also be prepared from complexes of lower volatility by solution impregnation employing a low-boiling organic solvent. In addition, metal carbonyls are easily decomposed directly to the metal under rather mild conditions. High temperatures, as required in preparing supported transition-metal catalysts from metal nitrate or chloride salts, are thus unnecessary. This improves the chances of achieving high metal dispersions even at relatively high metal concentrations.

We have recently begun to explore the possibility of preparing supported transition-metal catalysts from metal carbonyl complexes using photochemical methods. There are a number of potential advantages in using light-initiated processes here, since metal carbonyl complexes possess a very rich photochemistry. For example, mononuclear carbonyl complexes can oligomerize upon irradiation.[8] It may be possible then to prepare supported polynuclear complexes in a single step by irradiating the mononuclear complex in the presence of the support material. Multiple deligandations of metal carbonyls to highly unsaturated complexes[9,10] or even metal atoms[11,12] can also be photochemically induced. This may allow direct preparation of very small supported metal clusters via photodeligandation of metal cluster complexes, thereby avoiding a thermal decomposition step which could induce sintering. There are obstacles, however, that have thus far limited application of photochemical methods to the preparation of supported transition-metal catalysts.[13] The most obvious is the opacity of many traditional oxide support materials. At best, this drastically reduces the efficiency of any photochemical process due to a nearly complete loss of useful light to scattering and reflection or to absorption by the support. We have avoided this problem by employing a rather transparent silica as our support. By irradiating $Fe(CO)_5$ adsorbed on this material, we have successfully prepared supported $Fe_3(CO)_{12}$ in a single-step process. We describe our results in the following sections and propose a mechanism whereby $Fe_3(CO)_{12}$ is produced from sec-

---

(1) Pruett, R. L. *Science* (*Washington, D.C.*) **1981**, *211*, 11.

(2) Bailey, D. C.; Langer, S. H. *Chem Rev.* **1981**, *81*, 109.

(3) Brenner, A.; Hucul, D. A. *Inorg. Chem.* **1979**, *18*, 2836.

(4) Brenner, A.; Hucul, D. A.; Hardwick, S. J. *Inorg. Chem.* **1979**, *18*, 1478.

(5) Ballivet-Tkatchenko, D.; Coudurier, G. *Inorg. Chem.* **1979**, *18*, 558.

(6) Hucul, D. A.; Brenner, A. *J. Am. Chem. Soc.* **1981**, *103*, 217.

(7) Commeruc, D.; Chauvin, Y.; Hugues, F.; Basset, J. M.; Olivier, D. *J. Chem. Soc., Chem. Commun.* **1980**, 154.

(8) Geoffroy, G. L.; Wrighton, M. S. "Organometallic Photochemistry"; Academic Press: New York, 1979; p 34 ff.

(9) (a) Nathanson, G.; Gitlin, B.; Rosan, A. M.; Yardley, J. T. *J. Chem. Phys.* **1981**, *74*, 361. (b) Yardley, J. T.; Gitlin, B.; Nathanson, G.; Rosan, A. M. *Ibid.* **1981**, *74*, 370.

(10) Tumas, W.; Gitlin, B.; Rosan, A. M.; Yardley, J. T. *J. Am. Chem. Soc.* **1981**, *104*, 55.

(11) Karny, Z.; Naaman, R.; Zare, R. N. *Chem. Phys. Lett.* **1978**, *59*, 33.

(12) Hellner, L.; Masaret, J.; Vermeil, C. *Nouv. J. Chim.* **1979**, *3*, 721.

(13) A few reports have recently appeared regarding photochemical preparation of supported transition-metal catalysts, See: Nagy, N. B.; Eenoo, M. V.; Derouane, E. G. *J. Catal.* **1979**, *58*, 230. See also: Kinney, J. B.; Staley, R. H.; Reichel, C. L.; Wrighton, M. S. *J. Am. Chem. Soc.* **1981**, *103*, 4273.

0002-7863/82/1504-6590$01.25/0